Research Article

Jiali Zhang, Guangpu Zhao*, Na Li, Xue Gao, and Ying Zhang

Analyses of electrokinetic energy conversion for periodic electromagnetohydrodynamic (EMHD) nanofluid through the rectangular microchannel under the Hall effects

https://doi.org/10.1515/phys-2022-0201
received May 18, 2022; accepted August 17, 2022

Abstract: Two-dimensional electromagnetohydrodynamic behavior of nanofluids through rectangular microchannels is investigated. The combined effects of time-periodic pressure gradients and magnetic fields in terms of the Hall effects on nanofluid flow are considered. Under the Debye–Hückel linearization approximation, the semi-analytic solution of the velocity field is derived by Green's function method. Furthermore, the semi-analytic solutions of electrokinetic energy conversion (EKEC) efficiency and the streaming potential of nanofluids through the rectangular microchannels are obtained. The variations of the velocity, streaming potential, and EKEC efficiency with the electric double layer thickness K, Hartmann number Ha, Hall parameter m, and dimensionless frequency Ω are shown and briefly discussed.

Keywords: electrokinetic energy conversion efficiency, Hall effects, streaming potential, Green's function, nanofluids

1 Introduction

With the development of microfluidic technology, microfluidic chip or lab-on-a-chip, micro-electro-mechanical systems, micro nanotechnology, medical field, and biochemical analysis device have developed rapidly in the field of microfluidics and have wide application prospect [1–5]. At present, there are many microfluidic driving and control technologies, and the principles are different. The mechanisms commonly used to drive fluid flow in microtubes include pressure gradient, surface tension, electroosmotic force, Lorentz force, and electromagnetohydrodynamic (EMHD) effect [6–11].

In the microfluidic system, when the wall material of the microchannel contacts with the electrolyte solution, the wall will carry an electrostatic charge. The electrostatic charge attracts the opposite ions in the solution and repels the same ions, resulting in the rearrangement of ions near the wall to form an electric double layer (EDL) [12]. Under the pressure-driven condition, the ions in the EDL form a streaming current with the flow of the fluid [13]. With the flow of the fluid, ions accumulate downstream of the microchannel and eventually produce a potential difference, which is called streaming potential or streaming direction potential, and the direction is opposite to the flow direction of the fluid. The study of streaming potential has attracted the attention of many researchers [14–21]. In addition, the conversion of mechanical energy generated by fluid motion and chemical energy within the EDL into electrical energy is another important application of the streaming potential in microchannels [22]. This conversion process is called electrokinetic energy conversion (EKEC) efficiency. Many researchers have studied the EKEC efficiency of fluid through microchannels. Daiguji *et al.* [23] studied the EKEC efficiency in parallel plate nanofluidic channels. Wang and Kang [24] investigated the EKEC efficiency in silicon nanochannels. Chanda *et al.* [25] researched the EKEC efficiency in flexible micro-nanotubes and found that the EKEC efficiency of rigid pipes is relatively lower than that of flexible pipes. Jian *et al.* [26] investigated the EKEC efficiency of viscoelastic fluids passing through polyelectrolyte-grafted nanochannels under no-slip boundary conditions. Xie and Jian [27] were the first to investigate the EKEC efficiency of nanofluids and found that the introduction of nanoparticles could improve the

* **Corresponding author: Guangpu Zhao,** Department of Mathematics, College of Sciences, Inner Mongolia University of Technology, Hohhot, Inner Mongolia 010051, PR China, e-mail: zhaoguangpu105@sina.com
Jiali Zhang, Na Li, Xue Gao, Ying Zhang: Department of Mathematics, College of Sciences, Inner Mongolia University of Technology, Hohhot, Inner Mongolia 010051, PR China

energy conversion efficiency of fluids. Liu *et al.* [28] found that curved rectangular nanochannels could effectively improve the electrochemical mechanical energy conversion efficiency within a certain parameter range.

With the progress of science and technology, industrial automation technology is more and more widely used in various fields, and the Hall effect has a high sense of existence in all links of signal transmission and energy exchange of industrial automation technology, so it is particularly important in application technology. Hall effect is a kind of electromagnetic effect. When the current passes through the semiconductor perpendicular to the external magnetic field, the carrier will shift, and an additional electric field will be generated perpendicular to the direction of a current and magnetic field, resulting in a potential difference at both ends of the semiconductor. This phenomenon is the Hall effect. Shah *et al.* [29] studied the effects of electromagnetic hydrodynamics and the Hall effects on the compression of three-dimensional flow nanofluids between parallel rotating plates. Abbasi *et al.* [30] used the homotopy perturbation method to analyze the entropy generation of the creep of nanofluids with viscosity varying with temperature and the Hall effect. Krishna and Chamkha [31] studied the Hall and ion slip effects of viscoelastic fluid in magnetohydrodynamic convection between two rigid rotating plates with sinusoidal pressure gradient through porous media. Attia and Aboul-Hassan [32] studied the unsteady flow of viscous conductive fluid caused by the rotation of an infinite non-conductive porous disk under an axial uniform and constant magnetic field considering the Hall effects.

Therefore, based on previous literature, it is found that the EMHD of nanofluids passing through rectangular microchannels under unsteady conditions has rarely been studied [33,34]. This study aims to study the EMHD behavior of nanofluids passing through rectangular microchannels under the influence of the Hall effects with unsteady conditions, in which Green's function method is very effective to solve unsteady problems [35–38]. Therefore, we obtain the analytical solution of the velocity field using Green's function method and discuss the current potential and EKEC efficiency. It is hoped that this study can provide some help for the research of microfluidic systems and the EKEC efficiency and provide some reference value for future research.

2 Mathematical formulation

2.1 Problem definition

As shown in Figure 1, we consider that under the joint action of Z-direction uniform magnetic field B_0 and Y-direction pressure gradient flow, the incompressible viscous nanofluid passes through rectangular microchannels with width W and height H, and the wall potential of rectangular microchannels is ψ_0. The origin of the coordinate system is set at the lower-left corner of the rectangular microchannel. The flow is assumed to be unsteady, fully developed, and hydrodynamic. In addition, EDL formed by nanoparticles is not considered, and it is assumed that EDLs formed on the channel wall do not overlap in this study.

2.2 Electrical potential equation and approximate solution

For asymmetric ($z_+ = z_- = z$) electrolyte solution, the electrical potential $\Psi(X, Z)$ of the EDL, and the local volumetric net charge density $\rho_e(X, Z)$ are described by the following Poisson–Boltzmann (PB) equations [39]:

$$\frac{\partial^2 \Psi}{\partial X^2} + \frac{\partial^2 \Psi}{\partial Z^2} = -\frac{\rho_e(X, Z)}{\varepsilon}, \tag{1}$$

$$\rho_e(X, Z) = z_0 e(n_+ - n_-), \tag{2}$$

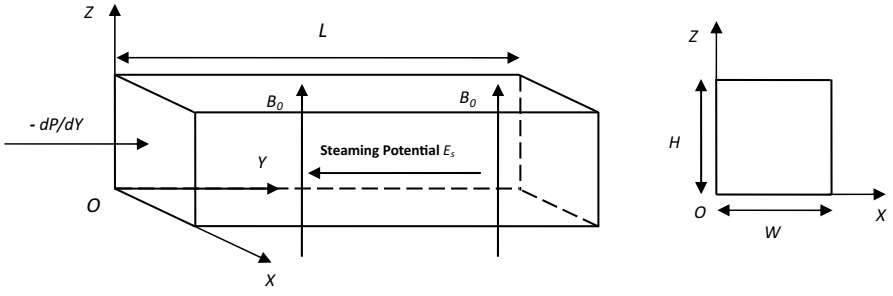

Figure 1: Geometry of the physical problem, coordinate system.

where ε is the fluid permittivity, z_0 is the valence number of ions, e is the elementary electric charge, n_+ and n_- are the number densities of the electrolyte cations and anions, respectively, and are given by the Boltzmann distribution, *i.e.*

$$n_{\pm} = n_0 \exp\left[\mp \frac{ez_0\Psi(X,Z)}{\kappa_B T_{av}}\right], \tag{3}$$

where n_0 is the bulk volume concentration of positive or negative ions which is independent of the surface electrochemistry, κ_B is the Boltzmann constant, and T_{av} is the absolute temperature over the entire channel. Assuming the electrical potential is small enough, the Debye–Hückel approximation can be employed for Eq. (3)

$$\exp\left[\mp \frac{ez\Psi(X,Z)}{\kappa_B T_{av}}\right] \approx 1 \mp \frac{ez\Psi(X,Z)}{\kappa_B T_{av}}. \tag{4}$$

Substituting Eqs. (3) and (4) into Eq. (2), we finally obtain

$$\rho_e(X,Z) = -2z_0 e n_0 \sinh\left(\frac{z_0 e\Psi(X,Z)}{\kappa_B T_{av}}\right). \tag{5}$$

The boundary conditions of the electrical potential are

$$\Psi|_{X=0} = \psi_0, \Psi|_{X=W} = \psi_0, \Psi|_{Z=0} = \psi_0, \Psi|_{Z=H} = \psi_0. \tag{6}$$

We introduce the following dimensionless variables

$$x = \frac{X}{H},\ z = \frac{Z}{H},\ \psi = \frac{\Psi}{\psi_0},\ K = \kappa H. \tag{7}$$

Under the condition that the double layer potential is small ($|\psi| < 1$), Eq. (1) can be linearized by the so-called Debye–Hückel approximation and we write Eq. (1) in dimensionless form as follows:

$$\frac{\partial^2\psi}{\partial x^2} + \frac{\partial^2\psi}{\partial z^2} = K^2\psi. \tag{8}$$

The boundary conditions are

$$\psi|_{x=0} = 1,\ \psi|_{x=\alpha} = 1,\ \psi|_{z=0} = 1,\ \psi|_{z=1} = 1, \tag{9}$$

where $\kappa = \left(\frac{2n_0 z_0^2 e^2}{\varepsilon\kappa_B T_{av}}\right)^{1/2}$ is the Debye–Hückel parameter and $1/\kappa$ denotes the thickness of the EDL and $\alpha = W/H$. The solution of Eq. (8) is subject to the boundary conditions Eq. (9) is

$$\psi(x,z) = \sum_{i=1}^{\infty} E_i \sin(\lambda_i x)\left[\sinh(\sqrt{\lambda_i^2 + K^2}z) + \frac{\sinh(\sqrt{\lambda_i^2 + K^2})}{1 - e^{-\sqrt{\lambda_i^2+K^2}}} e^{-\sqrt{\lambda_i^2+K^2}z}\right] + \sum_{j=1}^{\infty} F_j \sin(y_j z)\left[\sinh(\sqrt{y_j^2 + K^2}x) + \frac{\sinh(\sqrt{y_j^2 + K^2}\alpha)}{1 - e^{-\sqrt{y_j^2+K^2}\alpha}} e^{-\sqrt{y_j^2+K^2}x}\right], \tag{10}$$

where

$$E_i = \frac{2(1-(-1)^i)(e^{\sqrt{\lambda_i^2+K^2}} - 1)}{i\pi e^{\sqrt{\lambda_i^2+K^2}}\sinh(\sqrt{\lambda_i^2 + K^2})},\quad \lambda_i = \frac{i\pi}{\alpha}, \tag{11}$$

$i = 1, 2, 3,\ldots$

$$F_j = \frac{2(1-(-1)^j)(e^{\sqrt{y_j^2+K^2}\alpha} - 1)}{j\pi e^{\sqrt{y_j^2+K^2}\alpha}\sinh(\sqrt{y_j^2 + K^2}\alpha)},\quad y_j = j\pi, \tag{12}$$

$j = 1, 2, 3,\ldots$

2.3 Analytical solutions of the velocity field

The government equations for nanofluids flow can be expressed as [34,43]

$$\nabla\cdot\vec{U} = 0, \tag{13}$$

$$\rho_{eff}[\partial\vec{U}/\partial T + (\vec{U}\cdot\nabla)\vec{U}] = -\vec{\nabla}P + \mu_{eff}\nabla^2\vec{U} + \vec{F}, \tag{14}$$

where $\vec{U} = (V, U, W)$ is the flow velocity, T is the time, and ρ_{eff} is the effective density of the nanofluid, which is given by

$$\rho_{eff} = \varphi\rho_s + (1-\varphi)\rho_f, \tag{15}$$

where φ is the volume fraction of the nanoparticles, ρ_s is the density of a solid and ρ_f is the density of a fluid. μ_{eff} is the effective viscosity of the nanofluid, which is given by

$$\mu_{eff} = \frac{\mu_f}{(1-\varphi)^{2.5}}, \tag{16}$$

where μ_f is the viscosity of the base fluid. P is the pressure and $\vec{F}$ is the net body force acting on the fluid, which is essentially contributed by the interactions between the induced electrical field and the applied magnetic field. It is defined

$$\vec{F} = \rho_e(X,Z)\vec{E} + \vec{J}\times\vec{B}. \tag{17}$$

In general, the electric current density $\vec{J}$ is obtained from generalized Ohm's law for Hall effects, that is

$$\vec{J} = \sigma_{eff}(\vec{E} + \vec{U}\times\vec{B}) - \frac{\sigma_{eff}}{en_e}(\vec{J}\times\vec{B}), \tag{18}$$

where $\overrightarrow{E} = (0, E_s, 0)$, E_s is the intensity of induced electric field (streaming potential) along Y direction, $\overrightarrow{B}$ is the magnetic field along Z direction and its strength is B_0, σ_{eff} is the effective electrical conductivity of the nanofluid, which is given by

$$\sigma_{\text{eff}} = \sigma_f\left(1 + \frac{3(\sigma_s/\sigma_f - 1)\varphi}{(\sigma_s/\sigma_f + 2) - (\sigma_s/\sigma_f - 1)\varphi}\right), \tag{19}$$

where σ_s is the electrical conductivity of the nanoparticles, and σ_f is the electrical conductivity of base fluids. The flow is assumed unsteady and fully developed. Furthermore, due to the assumption of $H \ll L$, $W \ll L$, only the axial velocity component U (X, Z, T) of the rectangular microchannel along the Y-direction is considered. Hence, the corresponding Navier–Stokes equation governing the flow can be given as [43]

$$\begin{aligned}\rho_{\text{eff}}\frac{\partial U}{\partial T} = &-\frac{\mathrm{d}P}{\mathrm{d}Y} + \mu_{\text{eff}}\left(\frac{\partial^2 U}{\partial X^2} + \frac{\partial^2 U}{\partial Z^2}\right)\\ &+ \rho_e E_s - \frac{\sigma_{\text{eff}}B_0{}^2U - \sigma_{\text{eff}}{}^2B_0{}^2E_s/(en_e)}{1 + \sigma_{\text{eff}}{}^2B_0{}^2/(en_e)^2},\end{aligned} \tag{20}$$

where $-\mathrm{d}P/\mathrm{d}Y = \Omega' F(\omega T)$, Ω' is the amplitude, $E_s = E_1 F(\omega T)$. Now, as shown in Figure 1, square waveform periodic functions are introduced as follows [36]:

$$F(\omega T) = \frac{2}{\pi}\sum_{k=1}^{\infty}\frac{1 - \cos(k\pi)}{k}\sin(k\omega T). \tag{21}$$

The boundary conditions on the wall of the microchannel and initial conditions are

$$\begin{cases} U(X, Z, T)|_{X=0} = U(X, Z, T)|_{X=W} = 0\\ U_Z(X, Z, T) - \alpha_0 U(X, Z, T)|_{Z=0} = 0\\ U_Z(X, Z, T) + \alpha_1 U(X, Z, T)|_{Z=H} = 0\\ U(X, Z, T)|_{T=0} = 0. \end{cases} \tag{22}$$

Introducing the following dimensionless group:

$$\begin{aligned} &u = \frac{U}{U_e},\quad U_e = -\frac{\varepsilon\psi_0 E_0}{\mu_f},\quad U_p = \frac{\Omega' H^2}{\mu_f},\quad t = \frac{\mu_f}{\rho_f H^2}T,\\ &\mathrm{Ha} = B_0 H\sqrt{\frac{\sigma_f}{\mu_f}},\quad S = \frac{E_0 H}{U_e}\sqrt{\frac{\sigma_f}{\mu_f}},\quad \Omega = \frac{\rho_f H^2}{\mu_f}\omega,\\ &\bar{E}_s = \frac{E_s}{E_0},\quad m = \frac{\sigma_f B_0}{en_e},\quad u_r = \frac{U_p}{U_e}. \end{aligned} \tag{23}$$

where $\Omega' = -\mathrm{d}P/\mathrm{d}Y$, U_p is a reference pressure-driven flow velocity, U_e is the Helmholtz–Smoluchowski electroosmotic velocity, Ω is the dimensionless frequency. E_0 is the characteristic electric field, and K is the EDL thickness. Ha is the Hartmann number, which gives an estimate of the magnetic forces compared to the viscous forces. m is the Hall parameter. After inserting dimensionless parameters Eqs. (7) and (23) into Eq. (20), the dimensionless momentum equation, relevant boundary conditions, and initial conditions have the following form:

$$\begin{aligned}\frac{\partial u}{\partial t} = &a\left(\frac{\partial^2 u}{\partial x^2} + \frac{\partial^2 u}{\partial z^2}\right) - b\mathrm{Ha}^2 u\\ &+ \underbrace{cu_r F(\Omega t) - cK^2\psi\bar{E}_s + dm\mathrm{Ha}S\bar{E}_s}_{Q(x,z,t)},\end{aligned} \tag{24}$$

$$\begin{cases} u(x, z, t)|_{x=0} = u(x, z, t)|_{x=\alpha} = 0\\ u_z(x, z, t) - \alpha_0 u(x, z, t)|_{z=0} = 0\\ u_z(x, z, t) + \alpha_1 u(x, z, t)|_{z=1} = 0\\ u(x, z, t)|_{t=0} = 0, \end{cases} \tag{25}$$

where $a = c{\cdot}p$, $b = \frac{1}{1 + m^2q^2}qc$, $c = \frac{\rho_f}{\rho_{\text{eff}}}$, $d = bq$, $p = \frac{\mu_{\text{eff}}}{\mu_f}$, $q = \frac{\sigma_{\text{eff}}}{\sigma_f}$.

2.4 Solution produce

The non-dimensional energy Eq. (24) subject to the boundary conditions and initial conditions Eq. (25) is now solved using Green's function method. Green's function satisfies:

$$\begin{aligned}\frac{\partial g}{\partial t} = &a\left(\frac{\partial^2 g}{\partial x^2} + \frac{\partial^2 g}{\partial z^2}\right) - b\mathrm{Ha}^2 g\\ &+ \delta(x - \xi)\delta(z - \eta)\delta(t - \tau),\end{aligned} \tag{26}$$

subject to the following homogeneous boundary conditions and initial conditions:

$$\begin{cases} g(x, z, t|\xi, \eta, \tau)|_{x=0} = g(x, z, t|\xi, \eta, \tau)|_{x=\alpha} = 0\\ g_z(x, z, t|\xi, \eta, \tau) - \alpha_0 g(x, z, t|\xi, \eta, \tau)|_{z=0} = 0\\ g_z(x, z, t|\xi, \eta, \tau) + \alpha_1 g(x, z, t|\xi, \eta, \tau)|_{z=1} = 0\\ g(x, z, t|\xi, \eta, \tau)|_{t=0} = 0, \end{cases} \tag{27}$$

where $\delta(x)$ is the Dirac delta function. We begin with the Laplace transform Eq. (26)

$$\begin{aligned}sG = &a\left(\frac{\partial^2 G}{\partial x^2} + \frac{\partial^2 G}{\partial z^2}\right) - b\mathrm{Ha}^2 G\\ &+ \delta(x - \xi)\delta(z - \eta)\mathrm{e}^{-s\tau}.\end{aligned} \tag{28}$$

Assuming that $G(x, z, s|\ \xi, \eta, \tau)$ can be expressed in terms of the expansion

$$G(x, z, s|\xi, \eta, \tau) = \frac{2}{\alpha}\sum_{l=1}^{\infty}G_l(z|\eta)\sin\left(\frac{l\pi\xi}{\alpha}\right)\sin\left(\frac{l\pi x}{\alpha}\right). \tag{29}$$

show that $G_l(z|\eta)$ is governed by

$$\frac{\mathrm{d}^2G_l}{\mathrm{d}z^2} - \left(\frac{s + b\mathrm{Ha}^2}{a} + \frac{l^2\pi^2}{\alpha^2}\right)G_l = -\frac{\delta(z-\eta)}{a}\mathrm{e}^{-s\tau}, \quad (30)$$

$$\begin{cases} G_l'(0|\eta) - \alpha_0 G_l(0|\eta) = 0, \\ G_l'(1|\eta) + \alpha_1 G_l(1|\eta) = 0. \end{cases} \quad (31)$$

Consider the eigenfunctions

$$\begin{aligned} &\phi_n(z) = \beta_n \cos(\beta_n z) + \alpha_0 \sin(\beta_n z), \\ &n = 1, 2, 3, \ldots, \end{aligned} \quad (32)$$

Show that they satisfy the differential equation

$$\phi_n'' + {\beta_n}^2\phi_n = 0. \quad (33)$$

With the boundary conditions

$$\begin{cases} \phi_n'(0) - \alpha_0\phi_n(0) = 0, \\ \phi_n'(1) + \alpha_1\phi_n(1) = 0. \end{cases} \quad (34)$$

If β_n is chosen so that $(\alpha_0\alpha_1 - {\beta_n}^2) + (\alpha_0 + \alpha_1)\beta_n \cot(\beta_n) = 0$

Show that the solutions to the ordinary differential equation, we obtained as

$$G_l(z|\eta) = 2\mathrm{e}^{-s\tau}\sum_{n=1}^{\infty}\frac{\phi_n(\eta)\phi_n(z)}{q_n^2\left(s + b\mathrm{Ha}^2 + a\beta_n^2 + a\frac{l^2\pi^2}{\alpha^2}\right)}, \quad (35)$$

where

$$q_n^2 = \alpha_0^2 + \beta_n^2 + \frac{(\alpha_0 + \alpha_1)(\alpha_0\alpha_1 + \beta_n^2)}{\alpha_1^2 + \beta_n^2}. \quad (36)$$

Taking the inverse Laplace transform

$$\begin{aligned} &g(x, z, t|\xi, \eta, \tau) \\ &= \frac{4}{\alpha}H(t-\tau)\sum_{l=1}^{\infty}\sum_{n=1}^{\infty}\frac{\phi_n(\eta)\phi_n(z)}{q_n^2} \\ &\sin\left(\frac{l\pi\xi}{\alpha}\right)\sin\left(\frac{l\pi x}{\alpha}\right)\mathrm{e}^{-\left[a\left(\frac{l^2\pi^2}{\alpha^2}+\beta_n^2\right)+b\mathrm{Ha}^2\right](t-\tau)}, \end{aligned} \quad (37)$$

so, the dimensionless velocity profile is calculated by the following simplified formula:

$$u(x, z, t) = \int_0^t\int_0^1\int_0^{\alpha} Q(\xi, \eta, \tau)g(x, z, t|\xi, \eta, \tau)\mathrm{d}\xi\,\mathrm{d}\eta\mathrm{d}\tau, \quad (38)$$

where $Q(\xi, \eta, \tau)$ is defined in Eq. (24). The dimensionless velocity has been given by Eq. (38) and substituted into $Q(\xi, \eta, \tau)$ and Eq. (37) to obtain

$$\begin{aligned} u(x, z, t) = &\sum_{l=1}^{\infty}\sum_{n=1}^{\infty}\frac{4}{\alpha q_n^2}\phi_n(z)\sin\left(\frac{l\pi x}{\alpha}\right) \\ &\int_0^t F(\Omega\tau)H(t-\tau)\mathrm{e}^{-\left[a\left(\frac{l^2\pi^2}{\alpha^2}+\beta_n^2\right)+b\mathrm{Ha}^2\right](t-\tau)}\mathrm{d}\tau \\ &\cdot\left\{E_x(\mathrm{d}m\mathrm{Ha}S\int_0^1\phi_n(\eta)\mathrm{d}\eta\int_0^{\alpha}\sin\left(\frac{l\pi\xi}{\alpha}\right)\mathrm{d}\xi\right. \\ &- cK^2\int_0^1\int_0^{\alpha}\psi(\xi, \eta)\phi_n(\eta)\sin\left(\frac{l\pi\xi}{\alpha}\right)\mathrm{d}\xi\,\mathrm{d}\eta) \\ &\left. + cu_r\int_0^1\phi_n(\eta)\mathrm{d}\eta\int_0^{\alpha}\sin\left(\frac{l\pi\xi}{\alpha}\right)\mathrm{d}\xi\right\}, \end{aligned} \quad (39)$$

where $E_x = E_1/E_0$. It needs to be pointed out that the streaming potential (E_s) appearing in the above velocity field is unknown. It can be determined by setting the electro-neutrality condition as follows.

2.5 Calculation of the streaming potential

Due to the migration of excess free ions, the streaming potential or streaming current can also be generated by the Lorentz force. The accumulation of ions downstream can induce a conduction current I_c. To maintain the electroneutrality of the fluid system, the conduction current and the streaming maintain equilibrium in a steady state, *i.e.*, $I_c + I_s = 0$. Thus, the streaming potential (E_s) can be obtained.

$$I = ez_0\int_0^H\int_0^W(n_+U_+ - n_-U_-)\mathrm{d}X\mathrm{d}Z = I_s + I_c = 0, \quad (40)$$

where I_s is the streaming current, I_c is the conduction current, and $U_\pm$ is a combination of nanofluid advection velocity (U) and electromigrative velocity ($\pm ezE_s/f$), so that they can be written as

$$U_\pm = U \pm \frac{ez_0E_s}{f}. \quad (41)$$

In Eq. (41), f is the ionic friction coefficient. Substitute Eqs. (3), (39), and (41) into Eq. (40), we shall finally get the dimensionless streaming potential as

$$\bar{E}_s = \sum_{n=1}^{\infty}\sum_{l=1}^{\infty}\sum_{i=1}^{\infty}\sum_{j=1}^{\infty}\frac{R_{nl}A_{nlij}(u_rB_{1nl} - B_{2nlij} + B_{3nl})}{C}, \quad (42)$$

where A_{nlij}, B_{1nl}, B_{2nlij}, B_{3nl}, and C as follows:

$$A_{nlij} = \int_0^1 \int_0^\alpha \psi(\xi, \eta)\phi(\eta)\mathrm{d}\xi\,\mathrm{d}\eta, \tag{43}$$

$$B_{1nl} = c\int_0^1 \phi_n(\eta)\mathrm{d}\eta \int_0^\alpha \sin\left(\frac{l\pi\xi}{\alpha}\right)\mathrm{d}\xi, \tag{44}$$

$$B_{2nlij} = E_x cK^2 A_{nlij}, \tag{45}$$

$$B_{3nl} = E_x \mathrm{d}m\mathrm{Ha}S\int_0^1 \phi_n(\eta)\mathrm{d}\eta \int_0^\alpha \sin\left(\frac{l\pi\xi}{\alpha}\right)\mathrm{d}\xi, \tag{46}$$

$$C = \frac{\alpha e z_0 E_0}{fU_e}. \tag{47}$$

2.6 Efficiency of the EKEC

In the process of generating the streaming current (I_s) and the streaming electric field (E_s), the mechanical energy of the pressure-driven flow is converted to electric energy. The energy conversion efficiency ζ is defined as [40]:

$$\zeta = \left|\frac{P_{\mathrm{out}}}{P_{\mathrm{in}}}\right|, \tag{48}$$

where P_{in} and P_{out} respectively represent the input and output power, and the expression is

$$P_{\mathrm{in}} = \left|-\frac{\mathrm{d}P}{\mathrm{d}Y}Q_{\mathrm{in}}\right|, \tag{49}$$

$$P_{\mathrm{out}} = \left|\frac{I_s E_s}{4}\right|. \tag{50}$$

Here, Q_{in} denotes the flow rate for this pressure-driven flow and can be expressed as

$$Q_{\mathrm{in}} = \int_0^H \int_0^W U\mathrm{d}X\mathrm{d}Z, \tag{51}$$

$$I_s = ez_0\int_0^H \int_0^W U(n_+ - n_-)\mathrm{d}X\mathrm{d}Z, \tag{52}$$

we can get ζ from Eqs. (48)–(52) as

$$\zeta = \frac{1}{4}\frac{\alpha K^2 \bar{E}_s^{\,2}}{u_r \Gamma}\chi, \tag{53}$$

where $\chi = \frac{\mu_f e^2 z_0^2}{f\varepsilon}$, $\Gamma = \int_0^1\int_0^\alpha u\mathrm{d}x\mathrm{d}z$.

3 Results and discussion

In the previous section, the semi-analytic solutions were derived by Green's function method for velocity, the streaming potential, and EKEC efficiency of incompressible viscous nanofluid in a rectangular microchannel. They depend greatly on many dimensionless parameters defined earlier. To obtain interesting results, the practical ranges of these dimensionless parameters should be provided based upon pertinent physical variables [28,37,41,42]: H = 100 μm, T_{av} is 298 K, κ_{B} is $1.381 \times 10^{-23}\,\mathrm{J\,K^{-1}}$, $\varepsilon = 7 \times 10^{-10}\,\mathrm{C^2\,N^{-1}\,m^{-2}}$, $e = 1.6 \times 10^{-19}$ C, $z_0 = 1$, $\rho_s = 3{,}600\,\mathrm{kg\,m^{-3}}$, $\rho_f = 997.1\,\mathrm{kg\,m^{-3}}$, $\mu_f = 8.91 \times 10^{-3}\,\mathrm{kg\,m^{-1}\,s^{-1}}$, $\sigma_f = 0.05\,\mathrm{S\,m^{-1}}$, $\sigma_s = 10^{-12}\,\mathrm{S\,m^{-1}}$, $u_r = 1.0$, $\alpha = 1$, $\alpha_0 = 1$, $\alpha_1 = 1$, and $\varphi = 0.02$. The range of E_0 changes from 0.1 to $10^2\,\mathrm{V\,m^{-1}}$, f is taken as $10^{-12}\,\mathrm{N\,s\,m^{-1}}$, the range of the EDL thickness K changes from 10 to 45, the range of Ha changes from 0 to 10, the range of Ω changes from 10 to 120, and m is set to 0.4 to 1.2.

The numerical solution obtained by the Legendre–Gauss Quadrature method has been verified by the known available results given in the literature. The comparison of the mean flow velocity corresponding with the magnetic field is presented between the current study and the existing experimental data of Lemoff and Lee [44], and the theoretical results of Rivero and Cuevas's 2D model [45]. Through the comparison, it can be clearly found that the mean flow velocity of the fluid is evidently bigger than the values of the experimental data and theoretical results in the condition of m = 0.1, Ω = 300, and m = 1, Ω = 200. Because the intensity of the applied magnetic field is relatively small, consequently, the impacts of the Hall effects on the mean flow velocity are unremarkable. Furthermore, the bigger Hall parameter and smaller dimensionless frequency easily cause bigger mean flow velocity (Figure 2).

Figure 3 illuminates the variation of the dimensionless velocity with *x versus z* through the rectangular microchannel when t = 0.5 when the other parameters are fixed. In these figures, the Hall parameters are set to 0.8, 0.9, 1.0, and 1.1, respectively. As shown in Figure 3(a)–(d), the dimensionless velocity shows an overall increasing trend with the increase of the Hall parameter. It is also observed that there is an electroosmotic effect at the walls in the x-direction and z-direction. We find that with the increase of the Hall parameter, the dimensionless velocity at the wall in the x-direction increases gradually and the fluctuation is more and more obvious. The dimensionless velocity at the wall in the z-direction gradually decreases in a direction opposite to the fluid flow. This is because, with the increase of the Hall parameter, the conductivity and electromagnetic force of nanofluids increase, resulting

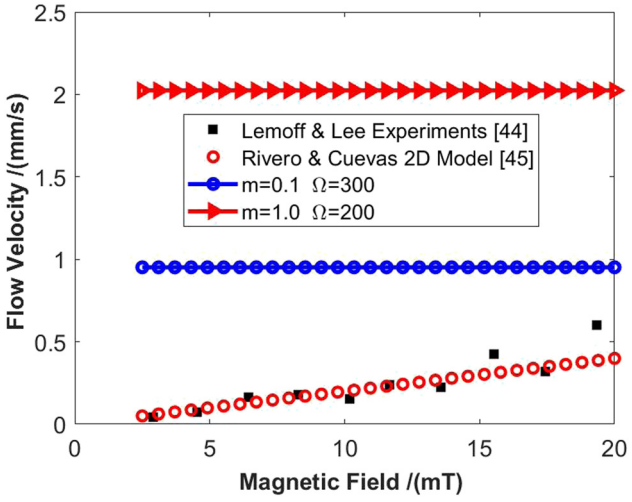

Figure 2: Comparison of the mean flow velocity of the present result with the existing experimental data of Lemoff and Lee [44] and the theoretical results of Rivero and Cuevas's 2D model [45].

in the corresponding increase of the dimensionless velocity of nanofluids.

Figure 4 depicts the variation of dimensionless velocity with x versus t at the cross-section of the rectangular microchannel when $z = 0.5$. In these figures, the dimensionless frequencies are set to 10, 20, 30, and 40, respectively. As shown in Figure 4(a)–(d), the larger the dimensionless frequency, the smaller the variation fluctuation period of dimensionless velocity with the increase of time. In addition, it can be seen that the overall velocity decrease with the increase in dimensionless frequency. This is because the larger the dimensionless frequency and the smaller the change period, the faster the fluid flow oscillation and the smaller the oscillation period, resulting in the incomplete development of the fluid and the smaller the amplitude, to reduce the dimensionless velocity.

Figure 5 illuminates the change of dimensionless velocity with z and t on the cross-section of rectangular microchannel at $x = 0.5$. The Hartmann numbers in Figure 5(a)–(d) are set to 2, 4, 6, and 8, respectively. It can be observed that the fluctuation of dimensionless velocity with time is different from that in Figure 4 due to different types of boundary conditions. In addition, it can be seen that the dimensionless velocity decreases with the increase of the Hartmann number. This is because the magnetic field hinders the flow of fluid. The larger the

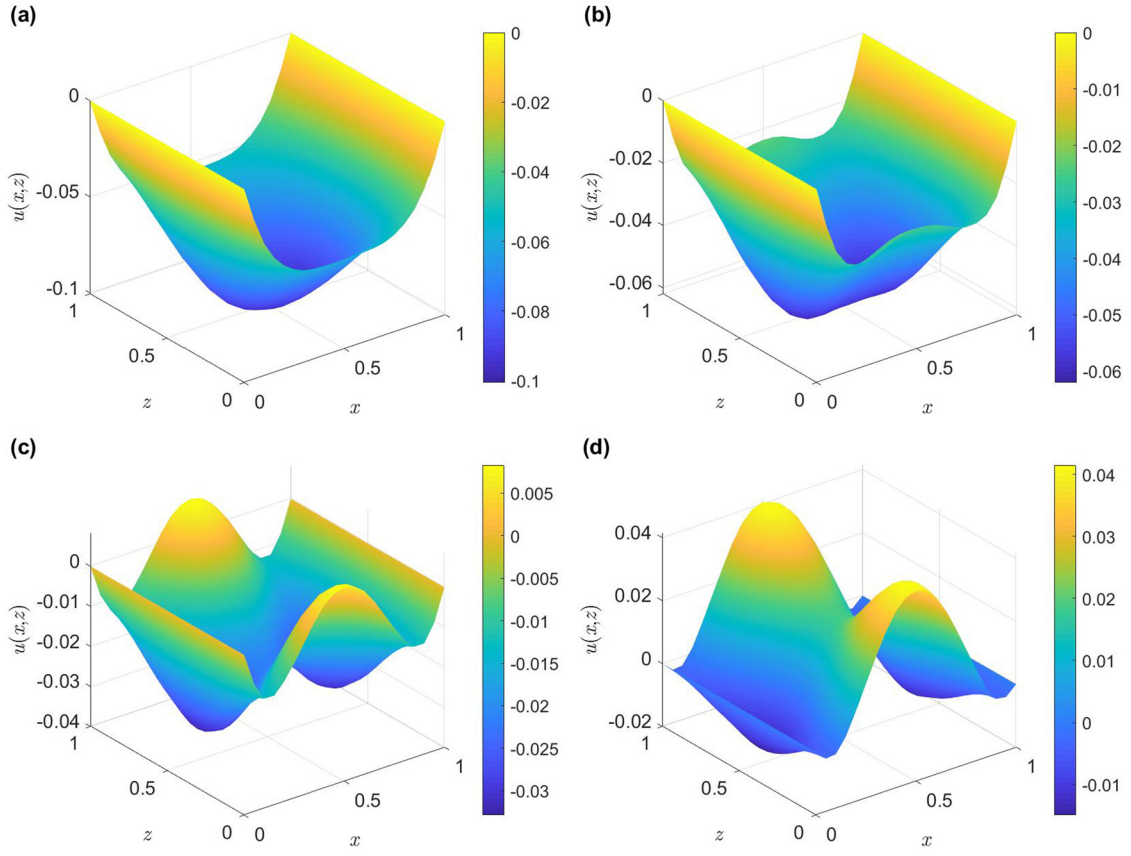

Figure 3: Dimensionless velocity distribution for $t = 0.5$ with (a) $m = 0.8$; (b) $m = 0.9$; (c) $m = 1.0$; and (d) $m = 1.1$ ($K = 10$, Ha = 5, $\Omega = 20$, $E_0 = 10$, $S = 5$).

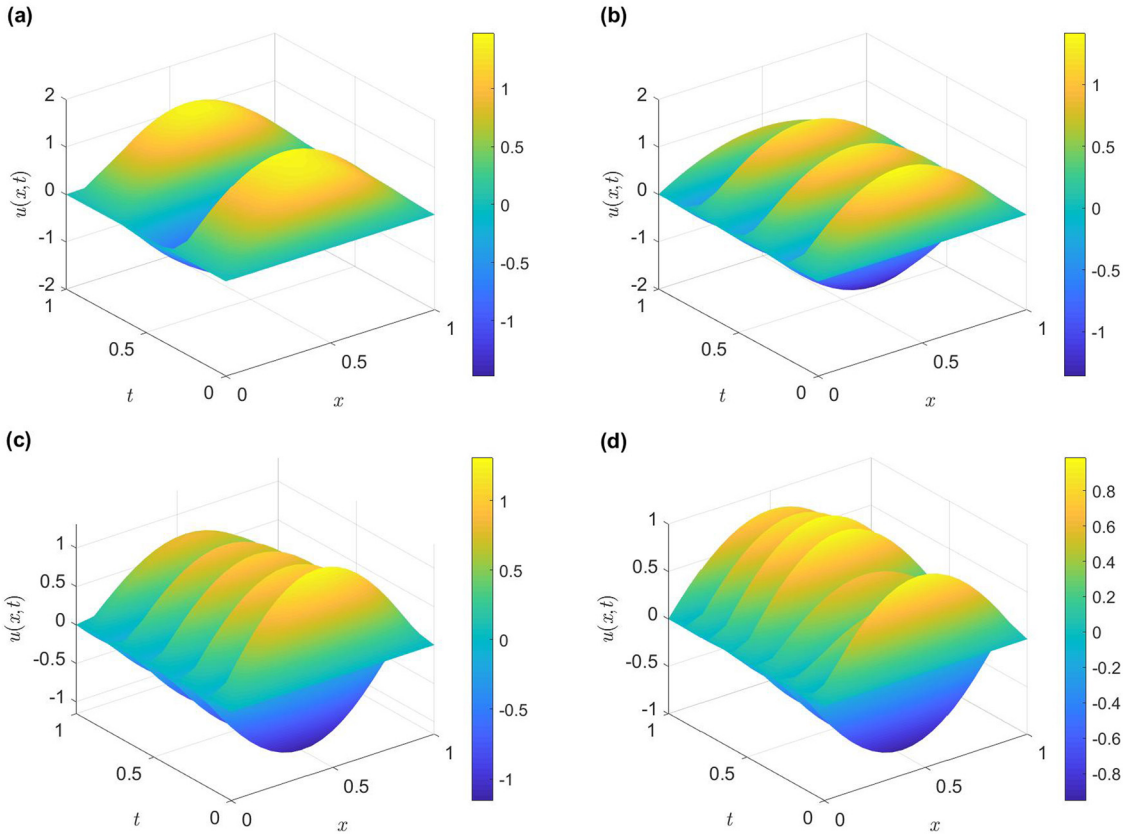

Figure 4: Dimensionless velocity distribution of the square waveform for $z = 0.5$ with (a) $\Omega = 10$; (b) $\Omega = 20$; (c) $\Omega = 30$; and (d) $\Omega = 40$ ($K = 20$, Ha = 5, $m = 1$, $E_0 = 10$, $S = 5$).

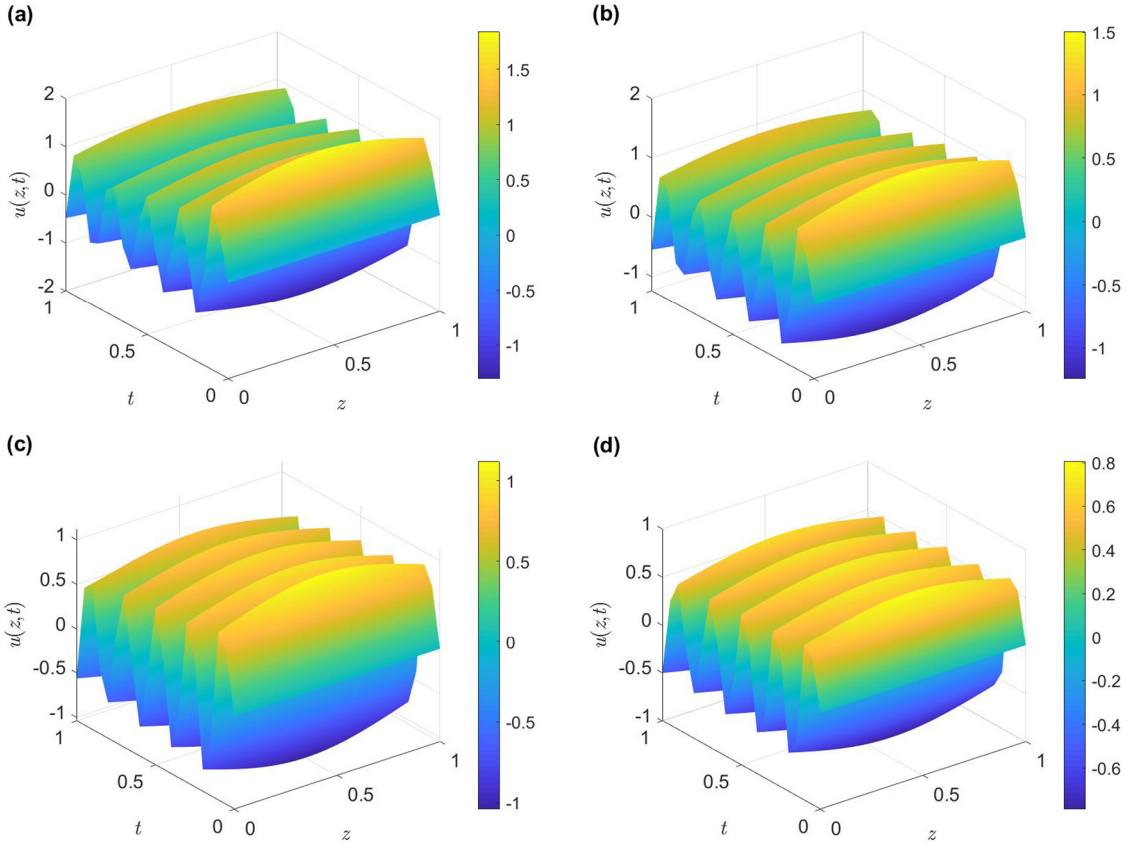

Figure 5: Dimensionless velocity distribution of the square waveform for $x = 0.5$ with (a) Ha = 2; (b) Ha = 4; (c) Ha = 6; and (d) Ha = 8. ($K = 15$, $m = 1$, $\Omega = 30$, $E_0 = 10$, $S = 5$).

Hartmann number, the greater the obstruction of fluid flow, and the smaller the amplitude of dimensionless velocity oscillation, thus reducing the flow velocity of nanofluid.

Figure 6 illustrates the variation of the dimensionless streaming potential for different EDL thickness K, Hall parameter m, Hartmann number Ha, and dimensionless frequency Ω with time. It can be observed that the variation of the dimensionless streaming potential with increasing time is in the form of simple harmonic wave motion. In addition, the dimensionless streaming potential, as shown in Figure 6(a), decreases as the dimensionless EDL thickness increases. This is because the thickness of the EDL decreases as K increases, and the number of free-charged ions in it decreases, thus causing a decrease in the streaming potential. As shown in Figure 6(b), the dimensionless streaming potential gradually decreases as the dimensionless frequency increases. This is because the higher the dimensionless frequency, the smaller the fluid flow period and the faster the oscillation, making it impossible for the fluid flow to fully develop, thus making the dimensionless streaming potential decrease. Figure 6(c) shows the larger the Hall parameter, the larger the dimensionless streaming potential. This is because the larger the Hall parameter, the greater the Hall effect produced. The presence of the Hall effects causes the streaming potential to increase as well. In Figure 6(d), the larger the Hartmann number, the smaller the streaming potential. This is because the larger Hartmann number means that the greater the blocking effect of the magnetic field on the flow of nanofluids (as shown in Figure 5), which leads to the reduction of the advection transport intensity of the ionic charges and hence the streaming potential decreases. In addition, we can observe that as the Hartmann number increases, the characteristics of the square waveform exhibited by changes in the streaming potential become more pronounced.

Figure 7 characterizes the variation of the EKEC efficiency with dimensionless time for different parameters such as EDL thickness, Hall parameters, Hartmann number, and dimensionless frequency. It is found that the EKEC efficiency fluctuates with time and that different parameters produce different effects. It is observed from

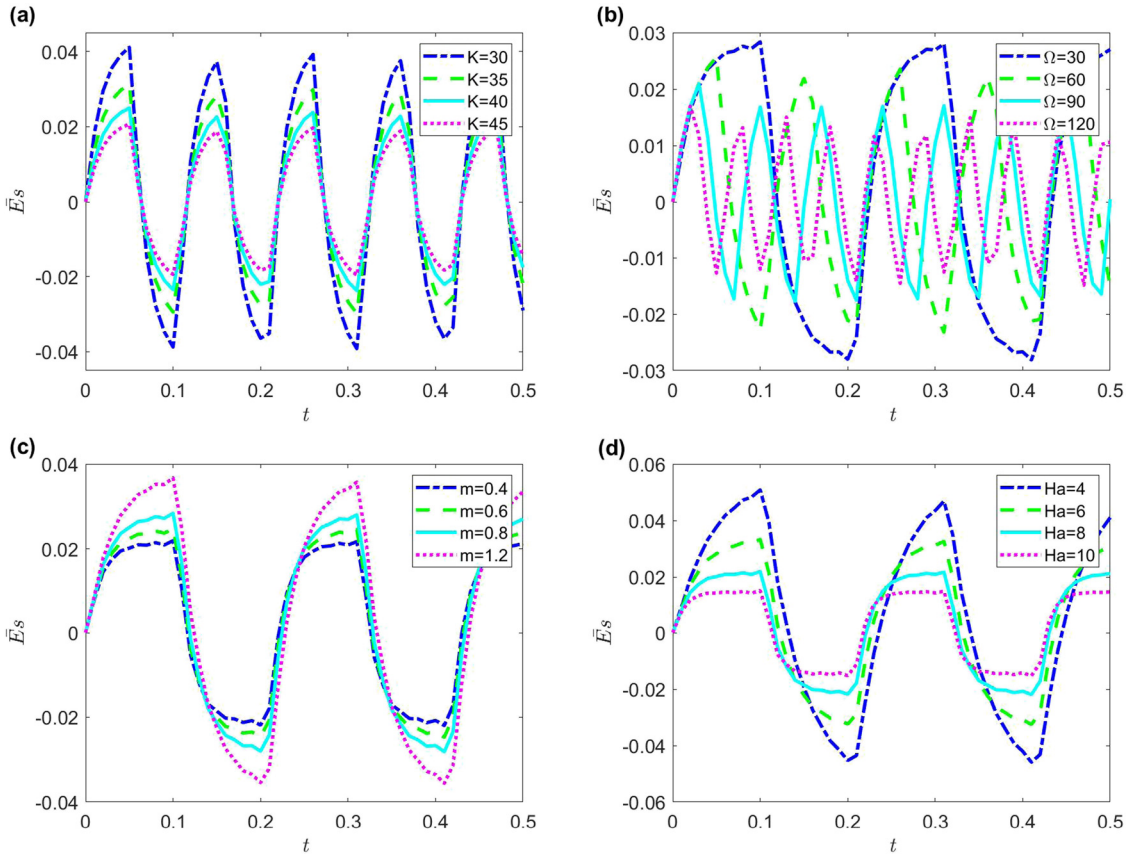

Figure 6: Variation of the dimensionless streaming potential with the dimensionless time for different values of (a) K when Ha = 8, m = 0.4, $E_0 = 10^2$, Ω = 60, S = 5; (b) dimensionless frequency Ω when K = 45, Ha = 8, m = 0.8, $E_0 = 10^2$, Ω = 30, S = 5; (c) Hall parameter m when K = 45, Ha = 8, $E_0 = 10^2$, Ω = 30, S = 5; and (d) Hartmann number Ha when K = 45, m = 0.4, $E_0 = 10^2$, Ω = 30, S = 5.

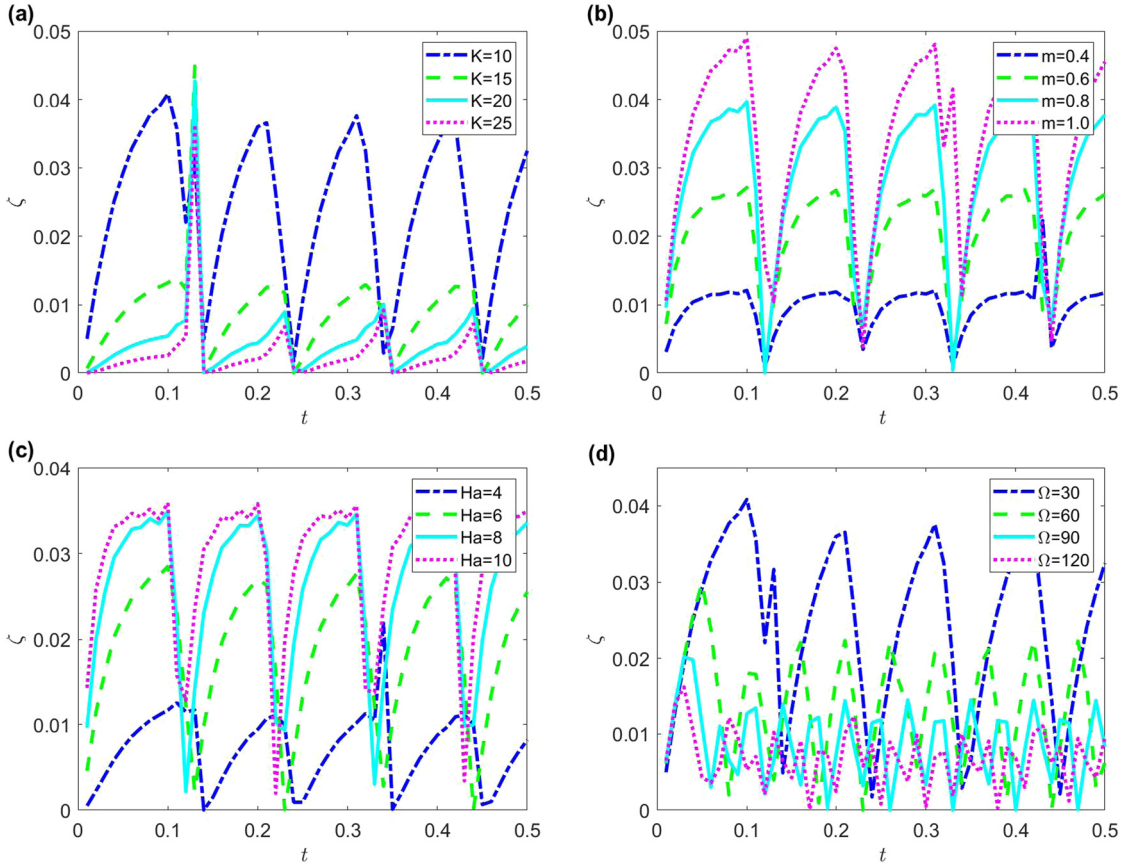

Figure 7: Variation of EKEC efficiency ζ with dimensionless time for different values (a) of the EDL thickness K when Ha = 6, $E_0 = 0.1$, $\Omega = 30$, $m = 1.2$, $S = 8$; (b) of Hall parameter m when $K = 10$, Ha = 8, $E_x = 0.1$, $\Omega = 30$, $S = 8$; (c) of Hartmann number Ha when $K = 10$, $m = 0.6$, $E_0 = 0.1$, $\Omega = 30$, $S = 9$; and (d) of dimensionless frequency Ω when $K = 10$, Ha = 6, $E_0 = 0.1$, $m = 1.2$, $S = 8$.

Figure 7(a) that the greater the EDL thickness, the smaller the EKEC efficiency. As shown in Figure 6(a), the dimensionless streaming potential decreases as the EDL thickness increases, which in turn makes the EKEC efficiency decrease. The results in Figure 7(b) show that the EKEC efficiency of the nanofluid increases as the Hall parameter becomes larger. This is because the larger the Hall parameter, the higher the conductivity and electromagnetic force of the nanofluid, which hinder the flow of the fluid. Therefore, in this process, the energy can be transformed more fully, and the greater the EKEC efficiency. Figure 7(c) shows that the larger the Hartmann number, the greater the EKEC efficiency. This explains that the larger the Hartmann number, the smaller the fluid flow velocity and the smaller the streaming potential. In this case, the streaming potential in Eq. (53) decreases more slowly relative to the velocity, and to some extent, they interact with each other, resulting in an increase in EKEC efficiency. Figure 7(d) shows that the larger the dimensionless frequency, the smaller the EKEC efficiency. This is explained as the larger the dimensionless frequency, the smaller the change fluctuation period of fluid flow, which makes the fluid velocity change and oscillate faster. In the process of fluid flow, the energy conversion is insufficient, which makes the electrokinetic conversion efficiency smaller.

4 Conclusions

This article analyzes the EMHD behavior of nanofluids through rectangular microchannels under the combined action of a magnetic field and pressure gradient under unsteady conditions. In addition, this study considers the influence of the Hall effect. Using Green's function method, the analytical solution of the velocity field of the nanofluid under the excitation of the square waveform is obtained. And further, the analytical solution of streaming potential and EKEC efficiency are obtained. The effects of the interaction among the Hartmann number Ha, Hall parameter m, dimensionless frequency Ω, EDL thickness K, and other

parameters on the velocity field, streaming potential and EKEC efficiency are qualitatively studied. It is observed that under certain parameters, the fluctuation of the streaming potential is in the form of a square waveform. And when other parameters are constant, a smaller EDL thickness, a smaller Hartmann number, and a smaller dimensionless frequency will all produce a larger streaming potential. On the contrary, the larger the Hall parameter, the greater the streaming potential is. In addition, the results also show that a larger Hall parameter and Hartmann number, a smaller EDL thickness and a dimensionless frequency can effectively improve the EKEC efficiency of the nanofluids.

Funding information: The work was supported by the National Natural Science Foundation of China (Grant No. 11802147) and the Foundation of Inner Mongolia Autonomous Region University Scientific Research Project (Grant No. NJZY18093).

Author contributions: All authors have accepted responsibility for the entire content of this manuscript and approved its submission.

Conflict of interest: The authors state no conflict of interest.

References

[1] Gravesen P, Branebjerg J, Jensen OS. Microfluidics-a review. J Micromech Microeng. 1993;3:168.
[2] Becker H, Gartner C. Polymer microfabrication methods for microfluidic analytical applications. Electrophoresis. 2000;21:12–26.
[3] Nandy K, Chaudhuri S, Ganguly R, Puri IK. Analytical model for the magnetophoretic capture of magnetic spheres in microfluidic devices. J Magn Magn Mater. 2000;320:1398–1405.
[4] Wang XQ, Mujumdar AS. Heat transfer characteristics of nanofluids:a review. Int J Therm Sci. 2007;46:1–19.
[5] Schoch RB, Han J, Renaud P. Transport phanomena in nanofluids. Rev Mod Phys. 2008;80:839.
[6] Squires TM, Quake SR. Microfluidics: fluid physics at the nanoliter scale. Rev Mod Phys. 2005;77:977–1026.
[7] Su J, Jian YJ, Chang L. Thermally fully developed electroosmotic flow through a rectangular microchannel. Int J Heat Mass Transf. 2012;55:6285–90.
[8] Buren MDL, Jian YJ, Chang L. Electromagnetohydrodynamic flow through a microparallel channel with corrugated walls. J Phys D. 2014;47:425501.
[9] Ma HC, Keh HJ. Diffusioosmosis of electrolyte solutions in a capillary slit with adsorbed polyelectrolyte layers. J Colloid Interface Sci. 2007;313:686–96.
[10] Jian YJ, Liu QS, Yang LG. AC electroosmotic flow of generalized Maxwell fluids in a rectangular microchannel. J Non-Newton Fluid. 2011;166:1304–14.
[11] Zhao GP, Jian YJ, Chang L, Buren MDL. Magnetohydrodynamic flow of generalized Maxwell fluids in a rectangular micropump under an AC electric field. J Magn Magn Mater. 2015;387:111–7.
[12] Hunter RJ. Zeta Potential in Colloid Science. London: Academic Press; 1981.
[13] Donath E, Voigt A. Streaming current and streaming potential on structured surfaces. J Colloid Interface Sci. 1986;109:122–39.
[14] Ren LQ, Qu WL, Li DQ. Interfacial electrokinetic effects on liquid flow in microchannels. Int J Heat Mass Transf. 2001;44:3125–34.
[15] Chakrabordy S, Das S. Streaming-field-induced convective transport and its influence on the electroviscous effects in narrow fluidic confinement beyond the Debye-Hückel limit. Phys Rev E. 2008;77:037303.
[16] Bharti RP, Harvie JE, Davidson M. Electroviscous effects in steady fully developed flow of a power-law liquid through a cylindrical microchannel. Int J Heat Fluid Flow. 2009;30:804–11.
[17] Chakraborty J, Ray S, Chakraborty S. Role of streaming potential on pulsating mass flow rate control in combined electroosmotic and pressure-driven microfluidic devices. Electrophoresis. 2012;33:419–25.
[18] Das S, Guha A, Mitra SK. Exploring new scaling regimes for streaming potential and electroviscous effects in a nanocapillary with overlapping electric double layers. Anal Chim Acta. 2013;804:159–66.
[19] Chen G, Dus S. Streaming potential and electroviscous effects in soft nanochannel beyond Debye-Hückel linearization. J Colloid Interface Sci. 2015;445:357–63.
[20] Vasu N, De S. Electroviscous effects in purely pressure driven flow and stationary plane analysis in electroosmotic flow of power-law fluids in a slit microchannel. Int J Eng Sci. 2010;48:1610–58.
[21] Matin MH. Electroviscous effects on the thermal transport of electrolytes in pressure driven flow through nanoslit. Int J Heat Mass Transf. 2017;106:473–81.
[22] Pennathur S, Eijkel JCT, Berg A. Energy conversion in Microsystems: is there a role for micro/nanofluidics. Lab Chip. 2007;7:1234–7.
[23] Daiguji H, Yang P, Szeri AJ, Majumdar A. Electrochemomechanical Energy conversion in Nanofluidic channels. Nano Lett. 2004;4:2315–21.
[24] Wang M, Kang Q. Electrochemomechanical energy conversion efficiency in silica nanochannels. Microfluid Nanofluidics. 2010;9:181–90.
[25] Chanda S, Sinha S, Das S. Streaming potential and electroviscous effects in soft nanochannels:towards designing more efficient nanofluidic electrochemomechanical energy converters. Soft Matter. 2014;10:7558–68.
[26] Jian YJ, Li FQ, Liu YB, Chang L, Liu QS, Yang LG. Electrokinetic energy conversion efficiency of viscoelastic fluids in a polyelectrolyte-grafted nanochannel. Colloids Surf B. 2017;156:405–13.
[27] Xie ZY, Jian YJ. Electrokinetic energy conversion in nanofluids in MHD-based microtube. Energy. 2020;212:118711.

[28] Liu YB, Jian YJ, Yang CH. Electrochemomechanical energy conversion efficiency in curved rectangular nanochannels. Energy. 2020;198:117401.
[29] Shah Z, Alzahrani EO, Alghamdi W, Ullah MZ. Influences of electrical MHD and Hall current on squeezing nanofluid flow inside rotating porous plates with viscous and joule dissipation. J Therm Anal Calorim. 2020;140:1215–27.
[30] Abbasi FM, Shanakhat I, Shehzad SA. Entropy generation analysis for peristalsis of nanofluid with temperature dependent viscosity and Hall effects. J Magn Magn Mater. 2019;474:434–41.
[31] Krishna MV, Chamkha AJ. Hall and ion slip effects on MHD rotating flow of elastico-viscous fluid through porous medium. Int Commun Heat Mass Transf. 2020;113:104494.
[32] Attia HA, Aboul-Hassan AL. Effect of Hall current on the unsteady MHD flow due to a rotating disk with uniform suction or injection. Appl Math Model. 2001;25:1089–98.
[33] Jian YJ, Liu QS, Yang LG. AC electroosmotic flow of generalized Maxwell fluids in a rechangular microchannel. J Non-Newton Fluid. 2011;166:1304–14.
[34] Yang CH, Jian YJ, Xie ZY, Li FQ. Heat transfer characteristics of magnetohydrodynamic electroosmotic flow in a rectangular microchannel. Eur J Mech B-Fluid. 2019;74:180–90.
[35] Kang Y, Yang C, Huang X. Dynamic aspects of electroosmotic flow in a cylindrical microcapillary. Int J Eng Sci. 2002;40:2203–21.
[36] Moghadam AJ. An exact solution of AC electro-kinetic-driven flow in a circular micro-channel. Eur J Mech B-Fluid. 2012;34:91–6.
[37] Moghadam AJ. Exact solution of AC electro-osmotic flow in a microannulus. J Fluid Eng-T ASME. 2013;135:091201
[38] Moghadam AJ. Effect of periodic excitation on alternating current electroosmotic flow in a microannulus channel. Eur J Mech B-Fluid. 2014;48:1–12.
[39] Chu X, Jian XJ. Magnetohydrodynamic electro-osmotic flow of Maxwell fluids with patterned charged surface in narrow confinements. J Phys D. 2019;52:405003.
[40] Bandopadhyny A, Chakraborty S. Giant augmentations in electro-hydro-dynamic energy conversion efficiencies of nanofluidic devices using viscoelastic fluids. Appl Phys Lett. 2012;101:043905.
[41] Jian YJ, Yang LG, Liu QS. Time periodic electro-osmotic flow through a microannulus. Phys Fluids. 2010;22:042001.
[42] Jing D, Bhushan B. Effect of boundary slip and surface charge on the pressure-driven flow. J Colloid Interface Sci. 2013;392:15–26.
[43] Zhao GP, Jian YJ, Li FQ. Streaming potential and heat transfer of nanofluids in microchannels in the presence of magnetic field. J Magn Magn Mater. 2016;407:75–82.
[44] Lemoff AV, Lee AP. An AC magnetohydrodynamic micropump. Sens Actuators B Chem. 2000;63:178–85.
[45] Rivero M, Cuevas S. Analysis of the slip condition in magnetohydrodynamic (MHD) micropumps. Sens Actuators B Chem. 2012;166–167:884–92.